Published in final edited form as:
Free Radic Biol Med. 2009 August 1; 47(3): 250–260. doi:10.1016/j.freeradbiomed.2009.04.018.

Radio-protective effects of manganese-containing superoxide dismutase mimics on ataxia telangiectasia cells

Julianne M. Pollard[1,2,3], **Julio S. Reboucas**[4], **Armando Durazo**[5], **Ivan Kos**[4], **Francesca Fike**[3], **Moeen Panni**[6], **Edith Butler Gralla**[5], **Joan Selverstone Valentine**[5], **Ines Batinic-Haberle**[4], and **Richard A. Gatti**[3,7]

[1]Department of Radiation Physics, University of Texas MD Anderson Cancer Center, Houston, TX 77030.

[2]Biomedical Physics Interdepartmental Graduate Program, The David Geffen School of Medicine at UCLA, CA 90095, USA

[3]Departments of Pathology and Laboratory Medicine and Human Genetics, The David Geffen School of Medicine at UCLA, CA 90095, USA

[4]Department of Radiation Oncology, Cancer Biology, Duke University Medical School, Durham, NC 27710, USA.

[5]Departments of Chemistry and Biochemistry, UCLA, Los Angeles, CA 90095-1569, USA.

[6]Department of Anesthesiology, University of Florida College of Medicine-Jacksonville, Jacksonville, FL 32209, USA.

[7]Department of Human Genetics, The David Geffen School of Medicine at UCLA, CA 90095, USA

Abstract

We tested several classes of antioxidant manganese compounds for radioprotective effects using human lymphoblastoid cells: six porphyrins, three salens and two cyclic polyamines. Radioprotection was evaluated by seven assays: XTT; Annexin V and propidium iodide flow cytometry analysis; γ-H2AX immunofluorescence; the neutral comet assay; dichlorofluorescein and dihydroethidium staining; resazurin and colony survival assay. Two compounds were most effective in protecting wildtype, and A-T cells, against radiation-induced damage: MnM_x-2-PyP-Calbio (a mixture of differently *N*-methylated MnT-2-PyP^+ from Calbiochem) and MnTnHex-2-PyP. MnTnHex-2-PyP protected WT cells against radiation-induced apoptosis by 58% (p=0.04) in WT by XTT and 39% (p=0.01) in A-T by Annexin V and propidium iodide staining. MnTnHex-2-PyP protected WT cells against DNA damage by 57% (p=0.005) by Gamma H2AX immunofluorescence and by 30% (p<0.01) by neutral comet assay. MnTnHex-2-PyP is more lipophilic than MnM_x-2-PyP-Calbio and is also >10-fold more SOD-active; consequently it is >50-fold more potent as a radioprotectant, as supported by six of the tests employed in this study. Thus, lipophilicity and antioxidant potency correlated with the magnitude of the beneficial radioprotectant effects observed. Our results identify a new class of porphyrinic radioprotectants for the general and radiosensitive populations and may also provide a new option for treating A-T patients.

Corresponding author. Tel.: +1 310 8257618.Fax +1 310 8257618 rgatti@mednet.ucla.edu.

Keywords

SOD mimics; ataxia telangiectasia; A-T, radioprotection; Mn porphyrins; AEOL10112; AEOL10113; Mn salens; Mn cyclic polyamines M40403; M40404; EUK-8; EUK-134; EUK-189

Introduction

Currently, no efficient radioprotectant is clinically available. Amifostine, approved by the US Food and Drug Administration in 1999, is still used in radiation oncology clinics but with low potency due to the stoichiometric nature of its action and very low bioavailibility [1,2]. Toxicity, severe nausea, allergy and acute hypotension have prompted a continuing search for better radioprotective compounds [2,3].

The ability of a compound to act as an antioxidant by quenching reactive oxygen species (ROS) is linked to its potential as a radioprotectant. This is not surprising given that the production of ROS is one indirect effect of radiation that can irrevocably damage DNA and lead to cell death in dividing cells. A number of radioprotective compounds have been identified that are antioxidants, such as Tempol (4-hydroxy-2,3,6,6-teramethyl piperidine-1-oxyl), vitamin E, and melatonin [2]. Tempol has been shown to protect against radiation-induced damage presumably due to its ability to abrogate ROS-mediated damage [4-7]. Pre-treatment of mice with Tempol prevented radiation-induced salivary gland function impairment [2,5,8].

Mn porphyrins are water-soluble, cell-permeable, and stable catalytic antioxidants [9-14]. Their protective effects have been associated with their ability to mimic superoxide dismutase (SOD) which reduces and oxidizes the superoxide radical; this produces hydrogen peroxide, which is then converted by catalase to H_2O and $O_2^{\cdot -}$. Compounds from this class were effective in several models of oxidative stress, such as small bowel ischemia/reperfusion, lung fibrosis, diabetes, and cancer [15-18]. **Mn salen compounds** possess SOD-like activity; however, this is abolished in the presence of EDTA, indicating that the low stability of such complexes may limit their antioxidant potency *in vivo* [19,20]. Both Mn porphyrins and Mn salen compounds also provide radioprotective effects [19,21-26]. **Mn cyclic polyamines** are potent SOD mimics in comparison to other classes of mimics, yet of fairly low metal/ligand stability which limits their *in vivo* utility [27,28].

Manganese SOD is a major component of the mitochondrial antioxidant defense system. Several animal models have been developed to investigate the role of Mn SOD in oxidative stress, neurodegenerative diseases and aging. *MnSOD2* deficient mice on a CD1 background have a foreshortened lifespan and display a multi-faceted phenotype including lipid accumulation in liver and skeletal muscle, a marked decrease in both succinate dehydrogenase and aconitase in the heart as well as metabolic acidosis and ketosis [29]. In addition, wildtype mice and murine cells treated with MnSOD gene therapy showed increased survival after radiation exposure compared to untreated mice and cells and reduced radiation-induced skin injury in mice [30,31]. Finally, studies have shown that heparin-SOD conjugate inhibits lung fibrosis after bleomycin exposure and EUK-189 increases survival of irradiated mice [32,33].

Synthetic antioxidants that would target mitochondria have been actively sought. Among compounds studied herein, MnTE-2-PyP was shown to distribute into mouse heart mitochondria after 10 mg/kg ip injection at levels high enough to protect it against peroxynitrite-mediated damage [34,35]. Work is in progress to prove our hypothesis that,

given its same antioxidant potency but higher lipophilicity, MnTnHex-2-PyP would distribute into mitochondria at an even higher level.

All SOD mimics employed in this study are Mn complexes and can release Mn to some degree, particularly when cycling between Mn(III) and Mn(II) during the dismutation process. Mn in its own right can dismute $O_2^{\cdot -}$ [11,20]; thus, $MnCl_2$ was used throughout as a control to account for possible SOD effects due to Mn release.

Individuals with Ataxia-Telangiectasia (A-T) comprise a group of patients that could benefit from both radioprotectants and antioxidants [36]. A-T is a rare neurodegenerative disorder with underlying immunodeficiency. These patients are also cancer-prone. Thus, they are frequently candidates for radiation therapy. However, because they are also sensitive to ionizing radiation, many adverse responses to radiation therapy have been reported over the past 40 years, including cases of mortality following standard radiation therapy [37-40]. The protein missing in A-T, Ataxia-Telangiectasia Mutated (ATM), is responsible for phosphorylating and, thereby, activating >900 DNA repair-related or cell cycle checkpoint proteins (i.e. p53, Chk2, SMC1, H2AX, Brca1 and Nbs1) following DNA damage [41-43]. In addition to radiation hypersensitivity, responses to oxidative stress are impaired. A-T patients have significantly decreased levels of total antioxidant capacity [44]. Studies performed in ATM-deficient mice reveal increased levels of nitric oxide-mediated damage, increased reactive oxygen species (ROS), and reduced catalase activity in neural cells [45]. Lymphoblastoid cells derived from A-T patients also display radiosensitivity, increased ROS and impaired mitochondrial function [46], making them a good laboratory model for identifying new radioprotectant compounds.

This is the first study where three different types of SOD mimics were compared for radioprotective effects. We compared the radioprotective effects of Mn porphyrins, Mn salen compounds, and Mn cyclic polyamines in human lymphoblastoid cells from both normals (wildtype) and A-T patients. Based on the 6 parameters studied, two of the Mn porphyrins (MnM_x-2-PyP-Calbio and MnTnHex-2-PyP) provided the most significant radioprotective effects.

MATERIALS AND METHODS

Cell culture and cell lines

Wildtype (WT) (derived from normal healthy individuals) and A-T lymphoblastoid cells were cultured in RPMI 1640 (Invitrogen) supplemented with 15% fetal bovine serum and 1% penicillin-streptomycin-glutamine at 37° C in a 5% CO_2 humidified chamber. All experiments were conducted in this medium unless otherwise indicated. A-T cells used varied from one experiment to another and included: for XTT, AT7LA, AT119LA, and AT224LA; for Annexin V/PI, AT119LA, AT223LA, and AT229LA; for neutral comet, AT227LA and AT229LA; for DCF and DHE, AT227LA, AT229LA, and AT234LA; and for resazurin, AT214LA and AT215LA.

Compounds/SOD Mimics

MnM_x-2-PyP-Calbio, purchased from Calbiochem (Batch# D00028286) as MnTM-2-PyP, was analyzed by thin-layer chromatography (TLC), uv/vis spectroscopy, cyclic voltammetry and ESI-MS; all indicated that it was not the compound originally claimed by Calbiochem. (The same was observed with a few batches of MnTE-2-PyP from the same source [47]). TLC indicated that it was a mixture of five different compounds (5 spots of similar intensity) of different hydrophilicities that correspond to nonmethylated and mono- to tetra-methylated compounds that are present in the mixture in similar amounts. All other analyses including mass spectroscopy and were in agreement with TLC data. Detailed analyses are described in

reference 47. The Mn porphyrins were synthesized and characterized as described [9,12]: MnTM-2-PyP [9,12]; MnTE-2-PyP [12,14]; MnTnHex-2-PyP [12]; MnTTEG-2-PyP [13] $MnBr_8TSPP$ [11]. $MnCl_2$ (Fisher) was used as a control for all compounds. The Eukaryon compounds: (EUK-8, EUK-134 and EUK-189) were obtained from Eukarion (Proteome Systems). The cyclic polyamines (M40403 and M40404) were synthesized as described previously [48].

$MnCl_2$ was used throughout the study as a control. Mn compounds, such as Mn salens and cyclic polyamines, can lose Mn *in vivo* either while redox-cycling with ROS and RNS when in a Mn^{+2} oxidation state or due to their low metal/ligand stability in both +2 and +3 oxidation states. Mn itself is known to be able to dismute superoxide [11,20,49,50]. $MnBr_8TSPP$ was recently proposed to protect SOD-deficient E. coli, based on its ability to transfer Mn to appropriate locations within the cell [11]. M40404 was reported as SOD-inactive and was used herein as a control for M40403 [27,48].

Assessment of the lipophilicity of the Mn compounds

Thin layer chromatography (TLC) was carried out on aluminum silica-gel sheets with fluorescent indicator (EMD Chemicals, Inc, 60 F_{254}) and eluted with a saturated $KNO_{3(aq)}$-H_2O-MeCN (1:1:8, v/v/v) mixture in a capped 1 L chamber. Typically, 1 μL of ~1 mM samples were applied at ~ 1cm of the strip border and the solvent front was allowed to run ~12 cm.

Irradiation

Cells were irradiated with a Mark I Cs^{37} irradiator at a dose rate of 5 Gy/min at room temperature. Radiation doses for each assay were determined by prior optimization.

Cytotoxicity: XTT

XTT, a tetrazolium salt, was used to measure cell viability after irradiation exposure. XTT is reduced by viable mitochondria to formazan, which causes a colorimetric change that can be measured at 450 nm. Approximately 5×10^4 cells were seeded per well in 96-well plates and incubated for 18 hours in fresh medium along with the compound at the final concentration indicated (3 replicates each). One set of plates was used as an unirradiated control and the other set was irradiated with 5 Gy. Five Gy was the optimal dose for observing efficient cytotoxicity within 48 hours. An XTT cell proliferation kit (Roche) was used to measure this cytotoxicity. All assays were performed in triplicate and the absorbance was read on a Spectramax plate reader.

Cytotoxicity: Annexin V/Propidium Iodide

Annexin V and propidium iodide staining were used as a second method to measure radiation-induced cytotoxicity. Cells were incubated in fresh medium along with the compounds at the final concentrations indicated. One set of samples was irradiated (5 Gy) to efficiently induce apoptosis within 48 hours. An annexin V/propidium iodide kit (BioVision) was used to detect apoptotic cells. The annexin V was labeled with fluorescein isothiocyanate (FITC) to detect phospholipid phosphatidylserine (PS) on the outer membrane of apoptotic cells; propidium iodide (PI) was used to detect necrotic cells. The assay was performed according to the manufacturer's instructions. Briefly, approximately 5×10^5 cells were washed in PBS, resuspended in annexin V and PI staining solution for 15 min at room temperature and analyzed immediately by flow cytometry (Flow Cytometry Core, UCLA).

DNA Damage : Gamma H2AX immunofluorescence

Radiation-induced DNA damage recognition was measured by γ-H2AX immunofluorescence. Wildtype (WT) cells were propagated in fresh medium with the compounds at specified concentrations. Only WT cells were used for this assay since irradiation does not induce formation of γ-H2AX foci in ATM-deficient cells [51]. WT cells were collected at log phase of their growth cycle, after an 18-hour incubation with the indicated compounds. After treatment, the cells were irradiated with 2 Gy and assessed at 15 minutes. These conditions maximized the yield of DNA damaged cells while minimizing cytotoxicity (Supplemental Figure 1). The cells were dropped onto coverslips and fixed with 4% paraformaldehyde, semi-permeabilized with 0.5% Triton-X 100 and washed with PBS. Cells were incubated with 1:400 dilution of mouse monoclonal antibody to γ-H2AX (Upstate Biotechnology), followed by 1:200 dilution of goat anti-mouse IgG antibody labeled with FITC (Jackson Immunochemicals) in PBS containing 10% FBS for 1.5 and 1 h, respectively. Slides were analyzed for γ-H2AX nuclear foci formation with FISH analysis software (Vysis) on a Leica DM RXA automated microscope equipped with Photometrix SenSyn. All slides were coded by one person and read blindly by another.

DNA Damage: Neutral comet assay

Neutral comet assay was used as another assessment of DNA damage. After an 18-hour incubation with the indicated compounds, human lymphoblastoid cells were irradiated with 10 Gy, then diluted 1:10 in 200 μl of 1% low melting point (LMP) agarose at 37°C . Aliquots (20 μl) of this mixture were cast into three replicate molds affixed to a Gelbond film (FMC Bioproducts, Rockport, ME) which was precoated with 1% normal melting point agarose in Tris-Borate-EDTA (TBE). Ten Gy was the lowest radiation dose that yielded consistently scorable neutral comets with our protocol (Supplemental Figure 2). The Gelbond films were incubated in lysis solution (2.5 M NaCl, 10 mM Tris, 100 mM Na_2EDTA, pH 10.0, with 1% v/v Triton X-100 and 10% DMSO added fresh) at the post-IR time points indicated, at 4°C overnight. The next day, the Gelbond films were removed from the lysis buffer, briefly rinsed with distilled water and then incubated in fresh, chilled electrophoresis buffer (300 mM NaOH and 1 mM EDTA, pH 13). After 2 hours at room temperature, to allow the DNA to unwind, electrophoresis was performed in TBE at 40V at 4°C for 2 hours. After electrophoresis the Gelbond film was washed three times at 4°C for 5 min each with neutralizing buffer (400 mM Tris-HCl, pH 7.5) before staining with SYBR Gold (1/10,000 dilution of stock solution from Molecular Probes, 495 nm excitation, 537 nm emission). The Gelbond film was rinsed with distilled water, incubated for 1 hour in ethanol, air dried overnight, and visualized using a Leica DM RXA automated microscope equipped with Photometrix SenSyn. Comets were measured with the Comet Score (TriTek Corp.) image analysis system.

ROS Assays

Intracellular ROS were measured using two probes: 2′-7′-dichlorofluorescein diacetate (DCFH-DA) (Invitrogen) and dihydroethidium (DHE) (Invitrogen). DCF was used as a general probe for ROS; DHE was used as a specific probe for superoxide [49]. DCFH-DA enters the cell and is easily hydrolysed by intracellular esterases to the non-fluorescent form DCFH which is rapidly converted to fluorescent DCF in the presence of a variety of ROS [52,53]. Upon oxidation by ROS, especially superoxide, DHE is converted to fluorescent ethidium bromide. For both assays, cells were plated in triplicate, pretreated overnight with the indicated compounds and incubated for 1 hour in PBS at 37°C with 10 μM of the indicated ROS probe. After incubation, the cells were rinsed briefly in PBS and the fluorescence intensity was measured by a Spectramax spectrophotometer. Irradiated samples were read by the spectrophotometer within 5 minutes after 10 Gy. Ten Gy was chosen due to the sensitivity of the assay (Supplemental Figures 3 and 4).

Mitochondrial Respiration Assay

The resazurin assay measures mitochondrial respiration [46]. Respiring mitochondria reduce resazurin to produce fluorescent resorufin. After an 18 hour incubation in the compounds indicated, 10^5 cells were plated in fresh medium along with resazurin at a final concentration of 3 μM. Each experiment was done in triplicate. Resazurin fluorescence was read at each hour for 3 hours on a Spectramax spectrophotometer.

Colony Survival Assay

The colony survival assay (CSA) was used to measure the effects of MnM_x-2-PyP-Calbio and MnTnHex-2-PyP on radiation-induced mitotic cell death. The CSA used in our lab has been designed to determine the in vitro radiosensitivity of patient cell lines in order to help diagnose potentially radiosensitive patients [54].During their logarithmic growth phase (1×10^6 cells/mL), cells were counted, treated with indicated compound overnight and plated at two cell concentrations (100 or 50 cells per well) in flat bottom 96-well plates in fresh media and split into two groups, irradiation and no irradiation. After plating, the irradiation plates were irradiated at the indicated radiation doses, then the plates were returned to the incubator for 10-13 days to grow. Finally, the cells were stained with a 0.1% solution in PBS of MTT dye (Sigma, St Louis, Mo) for at least 4 hours and the wells were counted under microscope. Wells with a colony of at least 32 cells were counted as positive wells. Colony-forming efficiency (CFE) was calculated as follows, CFE=(-ln F)/W, where F is the fraction of wells without colonies of 32 or more cells and W is the initial number of cells seeded per well. The resulting survival fraction (SF) after radiation exposure is calculated according to this formula, SF= 100 × (CFE of the irradiated plate)/(CFE of control 0 Gy plate). This assay was performed twice.

Statistics

Statistical analysis of all data was performed using Excel. P-values were determined using the Student's two-tailed T Test.

RESULTS

Radiation protection was evaluated by a reduction in radiation-induced cell death, apoptosis and/or DNA damage. We measured these three parameters to establish the radioprotectant potential of three classes of SOD mimics in WT and A-T cells in parallel to determine whether 1) any radioprotectant effects are dependent on ATM-related pathways, and 2) the compound(s) might have potential therapeutic benefits for radiosensitive patients. We noted radioprotective effects in 2 of the 11 compounds tested: MnM_x-2-PyP-Calbio and MnTnHex-2-PyP. Also, we noted possible ATM-dependent effects with three of the assays.

MnM_x-2-PyP and MnTnHex-2-PyP Increased Viability After Radiation Exposure

XTT was used to assess both the toxicity of the compounds and the effect of each compound on IR-induced cytotoxicity. All cells were pre-treated with the indicated compound two hours prior to being irradiated with 5 Gy and were assayed for viability 48 hours post-radiation. Three of the eleven tested compounds reduced IR-induced cytotoxicity in WT cells: MnM_x-2-PyP-Calbio, MnTnHex-2-PyP and $MnCl_2$ (Table 1). MnTnHex-2-PyP (1 μM) showed the most significant reduction in IR-induced cytotoxicity in WT cells, as compared to untreated irradiated WT cells: 58% (p=0.04). MnM_x-2-PyP-Calbio (56 μM) significantly reduced IR-induced cytotoxicity by 25% ($p= 6\times10^{-4}$) in WT cells. $MnCl_2$ (1 μM) was used as a control and reduced IR-induced cell death by 31% ($p=2 \times 10^{-5}$) in WT cells. None of the compounds exhibited any statistically significant reduction in IR-induced cytotoxicity in A-T cells.

MnM_x-2-PyP-Calbio, MnTnHex-2-PyP and EUK-134 Reduced IR-Induced Apoptosis

Annexin V and propidium iodide staining were used to measure post-radiation apoptosis. Three of the eleven compounds tested showed mild reduction in the percentage of apoptotic cells after radiation exposure: MnM_x-2-PyP, MnTnHex-2-PyP, and EUK-134 (Table 1). MnM_x-2-PyP-Calbio (56 μM) reduced IR-induced apoptosis by 11% (p=0.03) in WT cells. In A-T cells, MnTnHex-2-PyP (1 μM) reduced IR-induced apoptosis by 39% (p=0.01) and EUK-134 (10 μM) provided an 8% (p=0.03) protection against IR-induced apoptosis. The rest of the compounds showed no protection against IR-induced apoptosis. $MnCl_2$ showed no protection in either cell type.

MnTnHex-2-PyP Reduced IR-Induced γ-H2AX Immunofluorescence

DNA damage was measured by using immunofluorescence to detect the DNA double strand break (DSB) marker γ-H2AX. Three of the eleven chemicals reduced IR-induced γ-H2AX immunofluorescent nuclear foci (IRIFs). Unirradiated cells treated with MnTnHex-2-PyP showed evidence of slight toxicity at all doses; these cells were approximately 25% positive for IRIFs between 0.05 and 1 μM. Following irradiation (2 Gy), MnTnHex-2-PyP significantly reduced IRIFs in a dose dependent manner (Figure 2 A and B). Irradiated cells treated with vehicle alone were 72% positive for IRIFs. We observed a dose-dependent reduction with increasing concentrations, with the maximal effect at a final concentration of 1 μM (a 57% proportional decrease in IRIFs ($p=5 \times 10^{-3}$)). Similarly, EUK-134 (10 μM) caused a 52% proportional decrease in IRIF formation (p=0.06). The control, $MnCl_2$ (1 μM), showed no reduction in IRIFs. IRIF formation could not be studied in A-T cells.

MnM_x-2-PyP-Calbio and EUK-8 Reduced DNA Comet Tail Lengths in WT and A-T Cells

Irradiation-induced DNA damage and repair kinetics of DSBs were measured with the neutral comet assay. All cells were incubated with the compound indicated for 18 hours before being irradiated with 10 Gy. Lower IR doses failed to produce a sufficient amount of DNA damage that would allow any measureable effects. Thus, the 10 Gy was not intended as a clinically relevant perturbation but rather as a laboratory model for damaging DNA and following repair with or without the presence of radioprotective agents. In WT cells, repair of damage (indicated by the shortening of comets to pre-irradiation lengths) was completed by 2.5 hours post irradiation, while in A-T cells this was delayed for at least one hour longer (Figure 3.).

Ten of the eleven compounds reduced DNA comet tail lengths of WT cells. Treatment with both EUK-8 (10 μM) and MnM_x-2-PyP-Calbio (56 μM) significantly reduced comet tail length 20 minutes post–IR (10 Gy) by 30% ($p=1.9 \times 10^{-9}$) and 20% ($p=5.7 \times 10^{-5}$), respectively, in WT cells. Using A-T cells, only three compounds reduced comet tail lengths at 20 minutes post-IR: M40404 (20 μM) (28% reduction, $p=8.6\times10^{-3}$); MnTnHex-2-PyP (1 μM) (15 % reduction, $p=7.3\times10^{-3}$); and EUK-8 (20 μM) (16% reduction, $p=2.4\times10^{-4}$) (Table 1).

A-T Cells Exhibited Higher Levels of ROS than Wildtype and MnTnHex-2-PyP and MnM_x-2-PyP-Calbio Reduced IR-Induced ROS

DCF fluorescence was used to measure a variety of ROS, such as hydrogen peroxide and the hydroxyl radical (Figure 4). Unirradiated A-T cells showed a higher baseline level of ROS compared to unirradiated WT cells (p=0.001) (Figure 4A). Irradiated WT cells showed a slight increase in DCF fluorescence of 20% (p=0.02) 5 minutes after 10 Gy irradiation (Figure 4A). A-T cells did not show any significant increase in DCF fluorescence after radiation. Irradiated WT cells treated with the SOD mimics showed no significant decrease in ROS levels (Figure 4B). In contrast, treatment with MnTnHex-2-PyP (1 μM) and

MnM_x-2-PyP-Calbio (56 μM) significantly reduced ROS in irradiated A-T cells by 21% ($p=6.1 \times 10^{-9}$) and 8% ($p=2.0 \times 10^{-3}$), respectively (Figure 4C).

Superoxide radical formation was measured by DHE fluorescence (Figure 5). A-T cells showed an increased constitutive DHE fluorescence compared to WT cells ($p=1 \times 10^{-3}$) (Figure 5A). We noted a slight increase in DHE fluorescence after irradiation in WT cells ($p=5 \times 10^{-2}$). Treatment with MnTnHex-2-PyP (1 μM) and MnM_x-2-PyP-Calbio (56 μM) reduced DHE fluorescence after radiation exposure (10 Gy) for both cell types (Figure 5B and 5C). In irradiated WT cells, MnTnHex-2-PyP (1 μM) and MnM_x-2-PyP-Calbio (56 μM) reduced DHE fluorescence 5 minutes after radiation exposure by 14% ($p=1.6 \times 10^{-3}$) and 69% ($p=1.4 \times 10^{-13}$), respectively. For irradiated A-T cells, MnTnHex-2-PyP (1 μM) and MnM_x-2-PyP-Calbio (56 μM) reduced DHE fluorescence by 24% ($p=1.5 \times 10^{-7}$) and 47% ($p=2.2 - 10^{-12}$), respectively. Since these compounds are SOD mimics, we expected to see a reduction in superoxide formation after compound treatment and this was observed in both cell types. This was in contrast to the absence of antioxidant effects by these compounds on WT cells when assessed by DCF which is a general probe for multiple forms of ROS.

MnM_x-2-PyP-Calbio Treatment Improved Mitochondrial Respiration Rate of A -T Cells

A-T cells typically show a lower respiration rate than WT cells and this was noted in our experiments ($p=3.2 \times 10^{-2}$) [46]. When A-T cells were treated with 56 μM MnM_x-2-PyP-Calbio, mitochondrial respiration was improved (Figure 6). In fact, MnM_x-2-PyP-Calbio-treated A-T cells showed an increased metabolism of resazurin by 21.46 % which made treated A-T cells' resazurin profile nearly identical to that of WT cells ($p=9.7 \times 10^{-2}$). MnTnHex-2-PyP and EUK-8 were also tested for effects on mitochondrial respiration; we noted no effect.

MnM_x-2-PyP-Calbio nor MnTnHex-2-PyP Showed Any Protection Against Radiation-Induced Mitotic Cell Death

Cells were preconditioned with porphyrinic antioxidant to protect them in part against primary radiation insult. Two of the most protective compounds in the other assays, MnM_x-2-PyP-Calbio and MnTnHex-2-PyP, were used in the colony survival assay (CSA) to assess whether or not they could be used to reduce radiation-induced mitotic cell death. This assay addresses both the viability of a cell and its ability to remain functionally active and create colonies or clones. However, no statistically significant protection was conferred by either compound for both WT and A-T cells (Supplemental Data). No data is shown for WT cells treated with MnM_x-2-PyP-Calbio since this group of cells repeatedly failed to grow sufficient enough colonies to count. The lack of protection observed by the CSA is not surprising given that the other results seen in the other assays were noted within minutes to hours of radiation exposure, while CSA detects a long term effect. Also, for our CSA setup, the cells were only exposed to the indicated compounds from 12-18 hours and then placed in fresh media for 2 weeks. The compounds only had this 12-18 hour time frame to uptake the compound in order to create an effect on long-term colony formation. It is possible that had the compounds been continually replenished over the 2-week colony formation period, a statistically significant difference could have been observed. On the other hand, we noted quite the contrary; MnTnHex-2-PyP was mildly cytotoxic to W-T cells, but neither compound was cytotoxic to A-T cells (see Supplemental Figure 5).

Briefly summarized, we identified two SOD mimics that showed radioprotective effects in six of our assays: MnM_x-2-PyP-Calbio and MnTnHex-2-PyP. MnTnHex-2-PyP was approximately 50-fold more effective than MnM_x-2-PyP-Calbio overall. All compounds showed some beneficial effects in general DNA repair observed with the neutral comet

assay, including $MnCl_2$, suggesting that these SOD mimics all have the ability to inhibit indirect DNA damage. Although our XTT data showed 2 of the mimics being protective in WT cells exclusively, it is possible that this assay which requires mitochondrial break down of tetrazolium salt might not be well-suited for A-T cells which have been shown previously to exhibit a slower respiration rate [46]. This idea is supported by the fact that MnTnHex-2-PyP showed protection by XTT in WT, but not in A-T, yet showed protective effects in A-T but not WT cells in the Annexin V/PI assay, and the same compound was protective in both cell types by neutral comet assay. Additional studies will be necessary to clarify the exact role(s) of ATM in achieving the radioprotection measured by our assays.

DISCUSSION

We evaluated the effects of three classes of compounds on radiation-induced DNA damage and cytotoxicity, ROS formation and mitochondrial respiration. Our hypothesis was that a potential radioprotectant should be able to reduce radiation-induced DNA damage and subsequent cell death. The efficacy of the radioprotectant is likely mediated by its ability to act as an antioxidant; therefore, we sought to explore the effects of our compounds on ROS formation and mitochondrial respiration. Finally, we aimed to study whether these effects may be ATM-dependent.

This study is the first to compare different types of synthetic antioxidants. Six different **Mn porphyrins** were assayed for their ability to protect against radiation-induced cell damage and death in WT and radiosensitive A-T human lymphoblastoid cell lines. Based on radioprotective effects previously reported [22,24,25], we anticipated that Mn porphyrins would be very effective in protecting A-T cells.

We also studied the **Mn salen compounds** (i.e. EUK compounds) from Eukarion, Inc (Proteome Systems). The Mn salens have been used as cytoprotective and neuroprotective agents in rat models and in mice cardiac models [19,21,26]. They have also been used in a lung radioprotection study [23].

A third class of SOD mimics comprise the **cyclic polyamine-based SOD mimics**. M40403 has been shown to reverse endothelial function in apolipoprotein(E)-deficient mice and it has been shown to reduce hyperalgesia and inflammation in rats [27,28]. M40404 was reported not to possess the superoxide dimuting ability and was included in this study as a control [27].

Our results indicate that A-T cells appear to suffer from a dysregulation of oxidative stress, as suggested by many previous reports [41,44,45]. This can be potentially attributed to the impaired mitochondrial function leading to increased superoxide levels (Figures 5A, 5B and 6) [46]. Two of the SOD mimics, MnTnHex-2-PyP and MnM_x-2-PyP-Calbio, were able to significantly decrease levels of ROS both in the presence and absence of irradiation (Figures 4B, 5B and 5C). Also, MnM_x-2-PyP-Calbio, was able to increase the mitochondrial respiration of A-T cells to a rate similar to that of WT cells (Figure 6). This ability of the SOD mimics to abrogate ROS is highly relevant because the high levels of ROS in A-T patients have been implicated in the neurodegenerative phenotype [44,45,55-57].

In addition to our observation of increased ROS in A-T cells, we saw evidence for delayed DNA double-strand break repair that could only be abrogated to a limited extent by SOD mimic exposure (Figure 3A, 3B and Table 1). The important role of ATM in activating many DNA double-strand break repair proteins and cell cycle checkpoints during the first hour following DNA damage, provides a plausible mechanism for the hour-long lag in DNA repair observed in A-T cells compared to WT cells (Figures 3A and 3B).

MnM_x-2-PyP-Calbio and MnTnHex-2-PyP were able to reduce both IR-induced cell death and apoptosis. However, no such protective effect was observed by either compound in our CSA assay. Immediately upon irradiation, cells start to upregulate antiapoptotic inflammatory pathways which perpetuate primary oxidative damage. Our pre-IR drug incubation treatment of our cells for CSA perhaps did not allow them to fight secondary oxidative stress as a result of continuous upregulation of cellular transcriptional activity. We have recently observed the same effect in a stroke experiment where a continuous, but not single treatment, with Mn porphyrin was essential for a long-lasting protective effect [58]. Our rat pulmonary radiation experiments also suggest that in addition to primary oxidative stress, secondary stress accounts greatly for a resulting lung damage [59] thus a long-term presence of an antioxidant is critical. However, the scarcity of the MnM_x-2-PyP-Calbio compound due to Calbiochem's discontinuation of the product rendered it impossible to carry out further CSA experiments with both drugs under different conditions. The Calbiochem compound was only peripherally protective in our study and is practically difficult to reproduce its composition in our laboratories as it contained differently methylated porphyrins. Thus the effects of the continuous treatment of A-T cells before, during and after radiation with MnTnHex-2-PyP will be addressed in a subsequent study.

Across nearly all of the parameters studied MnM_x-2-PyP-Calbio and MnTnHex-2-PyP were the most effective radioprotectants. We tried to elucidate some of the mechanisms that might contribute to their efficacy. We assessed the lipophilicity of the Mn compounds studied. We employed thin-layer chromatography as a lipophilicity measure (Table 2). The most lipophilic compound (with highest R_f value) among Mn porphyrins was MnTnHex-2-PyP. The MnM_x-2-PyP-Calbio is fairly lipophilic also, and much more lipophilic than authentic MnTM-2-PyP and its ethyl analogue MnTE-2-PyP. Yet MnM_x-2-PyP-Calbio is a mixture of 5 different compounds which are present in similar amounts, non-methylated and mono to tetra-methylated. The presence of methyl groups affords thermodynamic and electrostatic facilitation of $O_2^{\cdot -}$ dismutation; thus, lack of methyl groups appears to decrease SOD-like potency. It could be anticipated, therefore, that MnM_x-2-PyP-Calbio is at least 10-fold less potent than MnTnHex-2-PyP (Table 3) [60]. This, along with the lower lipophilicity, contributes to its approximately 50-fold lesser efficacy than MnTnHex-2-PyP. In other words, at 56 μM, MnM_x-2-PyP-Calbio is still significantly less potent than 1 μM of MnTnHex-2-PyP. MnTM-2-PyP and MnTE-2-PyP are poor performers despite being as equally SOD-active as MnTnHex-2-PyP and they are significantly less lipophilic. Other compounds, although very lipophilic (e.g.Table 2) were ineffective in all assays other than in the neutral comet assay. Since $MnCl_2$ also speeds repair in the neutral comet assay, even at 1 μM level (20- or 56-times less than other compounds), it may be that some of the beneficial effects observed were due to Mn release from the fairly unstable Mn salens and Mn cyclic polyamines. Alternatively, the positive charge of the Mn porphyrin compounds may facilitate their localization to the mitochondria. If this localization is important, then the Mn salen and Mn cyclic polyamines, which do not bear strong positive charge, would be expected to be less effective even though their lipophilic nature allowed them to enter the cell. The importance of both positive charge and lipophilicity for mitochondrial accumulation has been nicely described and engineered by M. Murphy with MitoQ series of prospective drugs [61].

It is important to note that MnTnHex-2-PyP was chosen for this study based on its remarkable efficacy in other *in vivo* models of oxidative stress injuries where it was up to 120-fold more efficacious than MnTE-2-PyP. In rat pulmonary radioprotection it was protective in the range of 0.05 to 0.6 mg/kg [25]. It was further fully protective in SOD-specific model of aerobic growth of SOD-deficient *E. coli* at submicromolar levels [62] and in renal ischemia/reperfusion at 0.05 mg/kg [63]. Recently, MnTnHex-2-PyP was shown to nearly fully inhibit chronic morphine tolerance at 0.1 mg/kg [64]. Its increased efficacy

when compared to MnTE-2-PyP is predominantly due to its increased lipophilicity (Table 2) as they are otherwise of nearly identical SOD-like activity (Table 3). We were able to recently quantify the lipophilicity of Mn porphyrins with respect to their partition between n-octanol and water (P_{OW}) (which is a common measure of drug lipophilicity) and show that P_{OW} values are proportional to R_f values listed in Table 3 [65]. The toxicity of the hexyl compound was tested in mice *via* subcutaneous route. Toxicity was seen within few seconds of administering the dose to be tested, with severe shivers and hypotonia in the mice. The methodology used to estimate the TD_{50} (median toxic dose) was an up-down sequential allocation technique as described by Dixon and Massey [66] and resulting in an extremely accurate estimate of the median dose tested using discrete variable experiments. The TD_{50} dose was found to be 12.5 mg (+/− 2.8)/kg, which is up to 250-fold above the effective dose and allows thus a wide therapeutic window of this drug.

In conclusion, it appears that both SOD-like potency and lipophilicity contribute to the radioprotective effects seen. The effects observed with A-T cells give hope that perhaps these and other Mn porphyrins might be useful for reducing the neurodegenerative effects seen in A-T. In addition, once pharmacologically optimized, this class of compounds could be considered for the treatment of pulmonary failure [18], which accounts for roughly one-third of deaths in these patients [36]. SOD mimics may also confer radioprotection for A-T patients before they undergo radiation therapy or standard diagnostic radiologic procedures like computed tomography (CT).

Supplementary Material

Refer to Web version on PubMed Central for supplementary material.

Acknowledgments

This work was supported by US Public Health Grant NIH AI067769 (JMP and RAG) and grant NIH DK46828 (JSV and AD). IBH, IK and JSR acknowledge support of NIAID grant 5-U19-AI-067798-03 and the Wallace H. Coulter Translational Partners Grant Program. The authors also thank Dr. Rita Cantor for assistance with the statistical analyses for the ROS assays and Ms. Kelly Pettijohn for her assistance with the colony survival assay.

Abbreviations

A-T	Ataxia-telangiectasia
WT	wildtype
SOD	superoxide dismutase
IR	ionizing radiation
DSB	double strand break
IRIF	irradiation-induced immunofluorescent nuclear foci
MnTM-2-PyP^{5+}	manganese(III) tetrakis(*N*-methylpyridinium-2-yl) porphyrin (AEOL10112)
MnM$_x$-2-PyP^{z+}-Calbio	a mixture of differently *N*-methylated *ortho* isomers of MnTM-2-PyP$^+$ where the number of methyl groups, x, is 0-4 and the total charge of the molecule, z, is x+1
MnTE-2-PyP^{5+}	Mn(III) tetrakis (N-ethylpyridinium-2-yl) porphyrin (AEOL10113)
MnTnHex-2-PyP^{5+}	Mn (III) tetrakis(*N*-n-hexylpyridinium-2-yl) porphyrin

MnTTEG-2-PyP^{5+}	Mn (III) 5,10,15,20-tetrakis(N-(1-(2-(2(-2-methoxyethoxy)ethoxy)ethyl)pyridinium-2-yl) porphyrin
MnBr$_8$TSPP^{3-}	Mn (III) *beta*-octabromo-*meso*-tetrakis (4-sulfonatophenyl)porphyrin
EUK	Eukarion
DCF	dichlorofluorescein
DHE	dihydroethidium
XTT	2,3-bis(2-methoxy-4-nitro-5-sulfophenyl)-S-[(phenylamino)carbonyl]-2H-tetrazolium hydroxide. (In text, charges on compounds have been omitted for simplicity.)

References

1. Dest VM. Radioprotectants: Adding Quality of life to survivorship. Semin. Oncol. Nursing. 2006; 22:249–256.
2. Hosseinimehr SJ. Foundation review: trends in the development of radioprotective agents. Drug Disc. Today. 2007; 12:794–805.
3. Mabro M, Faivre S, Raymond E. A risk-benefit assessment of amifostine in cytoprotection. Drug Saf. 1999; 21:367–387. [PubMed: 10554052]
4. Baier JE, Neumann HA, Moeller T, Kissler M, Borchardt D, Ricken D. Radiation protection through cytokine release by N-acetylcysteine. Strahlenther Onkol. 1996; 172:91–98. [PubMed: 8669050]
5. Cotrim AP, Sowers AL, Lodde BM, Vitolo JM, Kingman A, Russo A, Mitchell JB, Baum BJ. Kinetics of tempol for prevention of xerostomia following head and neck irradiation in a mouse model. Clin. Cancer Res. 2005; 11:7564–7568. [PubMed: 16243832]
6. Wan XS, Ware JH, Zhou Z, Donahue JJ, Guan J, Kennedy AR. Protection against radiation-induced oxidative stress in cultured human epithelial cells by treatment with antioxidant agents. Int. J Rad. Oncol. Biol. Physics. 2006; 64:1475–1481.
7. Reliene R, Schiestl RH. Antioxidants suppress lymphoma and increase longevity in Atm-deficient mice. J Nutr. 2007; 137:229S–232S. [PubMed: 17182831]
8. Vitolo JM, Cotrim AP, Sowers AL, Russo A, Wellner RB, Pillemer SR, Mitchell JB, Baum BJ. The stable nitroxide tempol facilitates salivary gland protection during head and neck irradiation in a mouse model. Clin.Cancer Res. 2005; 10:1807–1812. [PubMed: 15014035]
9. Batinić-Haberle I, Benov L, Spasojević I, Fridovich I. The ortho effect makes manganese(III) meso-tetrakis(N-methylpyridinium-2-yl)porphyrin a powerful and potentially useful superoxide dismutase mimic. J Biol. Chem. 1998; 273:24521–24528. [PubMed: 9733746]
10. Ferrer-Sueta G, Batinić-Haberle I, Spasojević I, Fridovich I, Radi R. Catalytic scavenging of peroxynitrite by isomeric Mn(III) N-methylpyridylporphyrins in the presence of reductants. Chem. Res. Toxicol. 1999; 12:442–449. [PubMed: 10328755]
11. Rebouças JS, Defreitas-Silva G, Spasojević I, Idemori YM, Benov L, Batinić-Haberle I. Impact of electrostatics in redox modulation of oxidative stress by Mn porphyrins: Protection of SOD-deficient Escherichia coli via alternative mechanism where Mn porphyrin acts as a Mn carrier. Free Radic. Biol. Med. 2008; 45:201–210. [PubMed: 18457677]
12. Batinić-Haberle I, Spasojević I, Stevens RD, Hambright P, Fridovich I. Manganese(III) *meso*-tetrakis(*ortho*-*N*-alkylpyridyl)porphyrins. Synthesis, characterization, and catalysis of O_2^- dismutation. J. Chem. Soc., Dalton Trans. 2002; 13:2689–2696.
13. Batinić-Haberle I, Spasojević I, Stevens RD, Bondurant B, Okado-Matsumoto A, Fridovich I, Vujasković Z, Dewhirst MW. New PEG-ylated Mn(III) porphyrins approaching catalytic activity of SOD enzyme. Dalton Trans. 2006; 4:617–624. [PubMed: 16402149]
14. Spasojević I, Chen Y, Noel TJ, Fan P, Zhang L, Rebouças JS, St Clair DK, Batinić-Hberle I. Pharmacokinetics of the potent redox-modulating manganese porphyrin, MnTE-2-PyP(5+), in

plasma and major organs of B6C3F1 mice. Free Radic. Biol. Med. 2008; 45:943–949. [PubMed: 18598757]

15. Benov L, Batinić-Haberle I. A manganese porphyrin suppresses oxidative stress and extends the life span of streptozotocin-diabetic rats. Free Radic. Res. 2005; 39:81–88. [PubMed: 15875815]
16. Zhao Y, Chaiswing L, Oberley TD, Batinić-Haberle I, St Clair W, Epstein CJ, St Clair D. A mechanism-based antioxidant approach for the reduction of skin carcinogenesis. Cancer Res. 2005; 65:1401–1405. [PubMed: 15735027]
17. Watanabe T, Owada S, Kobayashi HP, Kawakami H, Nagaoka S, Murakami E, Ishiuchi A, Enomoto T, Jinnouchi Y, Sakurai J, Tobe N, Koizumi S, Shimamura T, Asakura T, Nakano H, Otsubo T. Protective effects of MnM2Py4P and Mn-salen against small bowel ischemia/reperfusion injury in rats using an in vivo and an ex vivo electron paramagnetic resonance technique with a spin probe. Transplant Proc. 2007; 39:3002–3006. [PubMed: 18089309]
18. Day BJ. Antioxidants as potential therapeutics for lung fibrosis. Antioxid. Redox. Signal. 2008; 10:355–370. [PubMed: 17999627]
19. Doctrow SR, Huffman K, Marcus CB, Tocco G, Malfroy E, Adinolfi CA, Kruk H, Baker K, Lazarowych N, Mascarenhas J, Malfroy B. Salen-manganese complexes as catalytic scavengers of hydrogen peroxide and cytoprotective agents: structure-activity relationship studies. J Med. Chem. 2002; 45:4549–4558. [PubMed: 12238934]
20. Spasojević I, Batinić-Haberle I, Stevens RD, Hambright P, Thorpe AN, Grodkowski J, Neta P, Fridovich I. Manganese(III) biliverdin IX dimethyl ester: a powerful catalytic scavenger of superoxide employing the Mn(III)/Mn(IV) redox couple. Inorg. Chem. 2001; 40:726–739. [PubMed: 11225116]
21. Musleh W, Bruce A, Malfroy B, Baudry M. Effects of EUK-8, a synthetic catalytic superoxide scavenger, on hypoxia- and acidosis-induced damage in hippocampal slices. Neuropharmacology. 1994; 33:929–934. [PubMed: 7969813]
22. Vujaskovic Z, Batinić-Haberle I, Rabbani ZN, Feng QF, Kang SK, Spasojević I, Samulski TV, Fridovich I, Dewhirst MW, Anscher MS. A small molecular weight catalytic metalloporphyrin antioxidant with superoxide dismutase (SOD) mimetic properties protects lungs from radiation-induced injury. Free Radic. Biol. Med. 2002; 33:857–863. [PubMed: 12208373]
23. Langan AR, Khan MA, Yeung IW, Van Dyk J, Hill RP. Partial volume rat lung irradiation: the protective/mitigating effects of Eukarion-189, a superoxide dismutase-catalase mimetic. Radiother. Oncol. 2006; 79:231–238. [PubMed: 16675053]
24. Rabbani ZN, Salahuddin FK, Yarmolenko P, Batinic-Haberle I, Thrasher BA, Gauter-Fleckenstein B, Dewhirst MW, Anscher MS, Vujaskovic Z. Low molecular weight catalytic metalloporphyrin antioxidant AEOL 10150 protects lungs from fractionated radiation. Free Radic. Res. 2007; 41:1273–1282. [PubMed: 17957541]
25. Gauter-Fleckenstein B, Fleckenstein K, Owzar K, Jiang C, Batinić-Haberle I, Vujaskovic Z. Comparison of two Mn porphyrin-based mimics of superoxide dismutase in pulmonary radioprotection. Free Radic. Biol Med. 2008; 44:982–989. [PubMed: 18082148]
26. van Empel VP, Bertrand AT, van Oort RJ, van der Nagel R, Engelen M, van Rijen HV, Doevendans PA, Crijns HJ, Ackerman SL, Sluiter W, De Windt LJ. EUK-8, a superoxide dismutase and catalase mimetic, reduces cardiac oxidative stress and ameliorates pressure overload-induced heart failure in the harlequin mouse mutant. J. Am. Coll. Cardiol. 2006; 48:824–832. [PubMed: 16904556]
27. Wang ZQ, Porreca F, Cuzzocrea S, Galen K, Lightfoot R, Masini E, Muscoli C, Mollace V, Ndengele M, Ischiropoulos H, Salvemini D. A newly identified role for superoxide in inflammatory pain. J Pharmacol. Exp. Ther. 2004; 309:869–878. [PubMed: 14988418]
28. Riley DP, Henke SL, Lennon PJ, Weiss RH, Neumann WL, Rivers WJ Jr. Aston KW, Sample KR, Rahman H, Ling CS, Shieh JJ, Busch DH, Szulbinksi W. Synthesis, characterization, and stability of manganese(II) C-substituted 1,4,,7,10,13-pentaazacyclopentadecane complexes exhibiting superoxide dismuting ability. Inorg. Chem. 1996; 35:5213–5231.
29. Huang TT, Carlson EJ, Raineri I, Gillespie AM, Kozy H, Epstein CJ. The use of transgenic and mutant mice to study oxygen free radical metabolism. Ann. N. Y. Acad. Sci. 1999; 893:95–112. [PubMed: 10672232]

30. Zhang X, Epperly MW, Kay MA, Chen ZY, Dixon T, Franicola D, Greenberger BA, Komanduri P, Greenberger JS. Radioprotection in vitro and in vivo by minicircle plasmid carrying the human manganese superoxide dismutase transgene. Hum Gene Ther. 2008; 19:820–826. [PubMed: 18699723]
31. Yan S, Brown SL, Kolozsvary A, Freytag SO, Lu M, Kim JH. Mitigation of radiation-induced skin injury by AAV2-mediated MnSOD gene therapy. J Gene Med. 2008; 10:1012–1018. [PubMed: 18613255]
32. Liu J, Wang X, Wang F, Teng L, Cao J. Attenuation effects of heparin-superoxide dismutase conjugate on bleomycin-induced lung fibrosis in vivo and radiation-induced inflammatory cytokine expression in vitro. Biomed Pharmacother. 2008 (Epublished ahead of print).
33. Srinivasan V, Doctrow S, Singh VK, Whitnall MH. Evaluation of EUK-189, a synthetic superoxide dismutase/catalase mimetic as a radiation countermeasure. Immunopharmacol Immunotoxicol. 2008; 30:271–290. [PubMed: 18569084]
34. Spasojević I, Chen Y, Noel TJ, Yu Y, Cole MP, Zhang L, Zhao Y, St Clair DK, Batinić-Haberle I. Mn porphyrin-based superoxide dismutase (SOD) mimic, MnIIITE-2-PyP5+, targets mouse heart mitochondria. Free Radic. Biol. Med. 2007; 42:1193–1200. [PubMed: 17382200]
35. Ferrer-Sueta G, Hannibal L, Batinic-Haberle I, Radi R. Reduction of manganese porphyrins by flavoenzymes and submitochondrial particles: a catalytic cycle for the reduction of peroxynitrite. Free Radic. Biol. Med. 2006; 41:503–512. [PubMed: 16843831]
36. Boder, E. Ataxia-telangiectasia: an overview. In: Gatti, RA.; Swift, M., editors. Ataxia-telangiectasia: genetics, neuropathology, and immunology of a degenerative disease of childhood. Alan R. Liss, Inc.; New York: 1985. p. 1-63.
37. Gotoff SP, Amirmokri E, Liebner EJ. Ataxia telangiectasia. Neoplasia, untoward response to x-irradiation, and tuberous sclerosis. Am. J Dis. Child. 1967; 114:617–25. [PubMed: 6072741]
38. Morgan JL, Holcomb TM, Morrissey RW. Radiation reaction in ataxia telangiectasia. Am. J Dis. Child. 1968; 116:557–558. [PubMed: 5687489]
39. Papageorgiou I, Paunier JP, Niederer J. Radiation therapy pneumonia. Radiol Clin. Biol. 1970; 39:256–261. [PubMed: 5475005]
40. Pollard, JM.; Gatti, RA. Clinical radiation sensitivity with DNA repair disorders: an overview. (submitted)
41. Shiloh Y. ATM and related protein kinases: safeguarding genome integrity. Nat. Rev. Cancer. 2003; 3:155–168. [PubMed: 12612651]
42. Matsuoka S, Ballif BA, Smogorzewska A, McDonald ER 3rd, Hurov KE, Luo J, Bakalarski CE, Zhao Z, Solimini N, Lerenthal Y, Shiloh Y, Gygi SP, Elledge SJ. ATM and ATR substrate analysis reveals extensive protein networks responsive to DNA damage. Science. 2007; 316:1160–1166. [PubMed: 17525332]
43. Bartek J, Bartkova J, Lukas J. DNA damage signalling guards against activated oncogenes and tumour progression. Oncogene. 2007; 26:7773–7779. [PubMed: 18066090]
44. Reichenbach J, Schubert R, Schindler D, Müller K, Böhles H, Zielen S. Elevated oxidative stress in patients with ataxia telangiectasia. Antioxid. Redox. Signal. 2002; 4:465–469. [PubMed: 12215213]
45. Barzilai A, Yamamoto K. DNA damage responses to oxidative stress. DNA Repair (Amst). 2004; 3:1109–1115. [PubMed: 15279799]
46. Ambrose M, Goldstine JV, Gatti RA. Intrinsic mitochondrial dysfunction in ATM-deficient lymphoblastoid cells. Hum. Mol. Genet. 2007; 16:2154–2164. [PubMed: 17606465]
47. Reboucas JS, Spasojević I, Batinić-Haberle I. Quality of Mn-porphyrin-based SOD mimics and peroxynitrite scavengers for preclinical mechanistic/therapeutic purposes. J. Pharm. Biomed. Anal. 2008; 48:1046–1049. [PubMed: 18804338]
48. Aston K, Rath N, Naik A, Slomczynska U, Schall OF, Riley DP. Computer-aided design (CAD) of Mn(II) complexes: superoxide dismutase mimetics with catalytic activity exceeding the native enzyme. Inorg. Chem. 2001; 40:1779–89. [PubMed: 11312732]
49. Archibald FS, Fridovich I. The scavenging of superoxide radical by manganous complexes: In vitro. Archives of Biochemistry and Biophysics. 1982; 214:452–463. [PubMed: 6284026]

50. Al-Maghrebi M, Fridovich I, Benov L. Manganese Supplementation Relieves the Phenotypic Deficits Seen in Superoxide-dismutase-null Escherichia coli. Arch. Biochem. Biophys. 2002; 402:140–109.
51. Rogaku EP, Pilch DR, Orr AH, Ivanova VS, Bonner WM. DNA double-stranded breaks induce histone H2AX phosphorylation on serine 139. J. Biol. Chem. 1998; 273:5858–5868. [PubMed: 9488723]
52. Royall JA, Ischiropoulos H. Evaluation of 2′,7′-dichlorofluorescin and dihydrorhodamine 123 as fluorescent probes for intracellular H2O2 in cultured endothelial cells. Arch. Biochem. Biophys. 1993; 302:348–355. [PubMed: 8387741]
53. Halliwell B, Whiteman M. Measuring reactive species and oxidative damage in vivo and in cell culture: how should you do it and what do the results mean? Br J Pharmacol. 2004; 142:231–255. [PubMed: 15155533]
54. Sun X, Becker-Catania SG, Chun HH, Hwang MJ, Huo Y, Wang Z, Mitui M, Sanal O, Chessa L, Crandall B, Gatti RA. Early diagnosis of ataxia-telangiectasia using radiosensitivity testing. J Pediatr. Jun; 2002 140(6):724–31. [PubMed: 12072877]
55. Jiang F, Guo Y, Salvemini D, Dusting GJ. Superoxide dismutase mimetic M40403 improves endothelial function in apolipoprotein(E)-deficient mice. Br. J. Pharmacol. 2003; 139:1059–1060. [PubMed: 12871823]
56. Kamsler A, Daily D, Hochman A, Stern N, Shiloh Y, Rotman G, Barzilai A. Increased oxidative stress in ataxia telangiectasia evidenced by alterations in redox state of brains from Atm-deficient mice. Cancer Res. 2001; 61:1849–1854. [PubMed: 11280737]
57. Yi M, Rosin MP, Anderson CK. Response of fibroblast cultures from ataxia-telangiectasia patients to oxidative stress. Cancer Lett. 1990; 54:43–50. [PubMed: 2208088]
58. Sheng, H.; Sakai, H.; Yang, W.; Fukuda, S.; Salahi, M.; Day, BJ.; Huang, J.; Paschen, W.; Batinic-Haberle, I.; Crapo, JD.; Pearlstein, RD.; Warner, DS. Sustained treatment is required to produce long-term neuroprotective efficacy from a metalloporphyrin catalytic antioxidant in focal cerebral ischemia. (submitted)
59. Gauter-Fleckenstein, B.; Batinic-Haberle, I.; Fleckenstein, K.; Vujaskovic, Z. Early and late administration of antioxidant mimetic MnTE-2-PyP5+ in mitigation and treatment of radiation-induced lung damage. ASTRO and RRS Meeting; Boston. 2008;
60. Batinic-Haberle I, Spasojevic I, Hambright P, Benov L, Crumbliss AL, Fridovich I. The relationship between redox potentials, proton dissociation constants of pyrrolic nitrogens, and in vitro and in vivo superoxide dismutase activities of manganese(III) and iron(III) cationic and anionic porphyrins. Inorg. Chem. 1999; 38:4011–4022.
61. Murphy MP. Targeting lipophilic cations to mitochondria. Biochim. Biophys. Acta. 2008; 177:1028–1031. [PubMed: 18439417]
62. Okado-Matsumoto A, Batinic-Haberle I, Fridovich I. Complementation of SOD-deficient Escheria Coli by manganese porphyrin mimics of superoxide dismutase activity. Free Radic. Biol. Med. 2004; 37:401–10. [PubMed: 15223074]
63. Saba H, Batinić-Haberle I, Munusamy S, Mitchell T, Lichti C, Megyesi J, MacMillan-Crow LA. Manganese porphyrin reduces renal injury and mitochondrial damage during ischemia/reperfusion. Free Radic. Biol. Med. 2007; 42:1571–1578. [PubMed: 17448904]
64. Batinić-Haberle I, Ndengele MM, Cuzzocrea S, Rebouças JS, Spasojević I, Salvemini D. Lipophilicity is a critical parameter that dominates the efficacy of metalloporphyrins in blocking morphine tolerance through peroxynitrite-mediated pathways. Free Radic. Biol. Med. 2009; 46:212–219. [PubMed: 18983908]
65. Kos I, Reboucas JS, DeFreitas-Silva G, Vujaskovic Z, Dewhirst MW, Spasojevic I, Batinic-Haberle I. The effect of lipophilicity of porphyrin-based antioxidants. Comparison of ortho and meta isomers of Mn(III) N-alkylpyridylporphyrins. Free Radic Biol Med. 2009 submitted.
66. Dixon, WJ.; Massey, FJ. Introduction to Statistical Analysis. 4th edition. McGraw-Hill; New York: 1983. p. 428-439.
67. Maroz A, Kelso GF, Smith RAJ, Ware DC, Anderson RF. Pulse radiolysis investigation on the mechanism of the catalytic action of Mn(II)-pentaazamacrocycle compounds as superoxide dismutase mimics. J. Phys. Chem. 2008; 112:4929–4935.

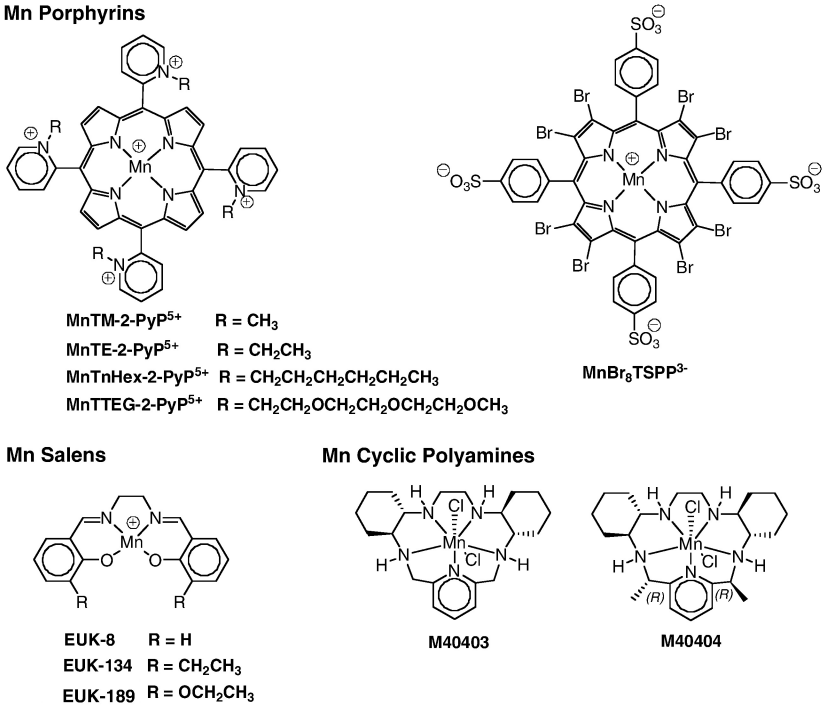

Figure 1.
Structures of Mn compounds

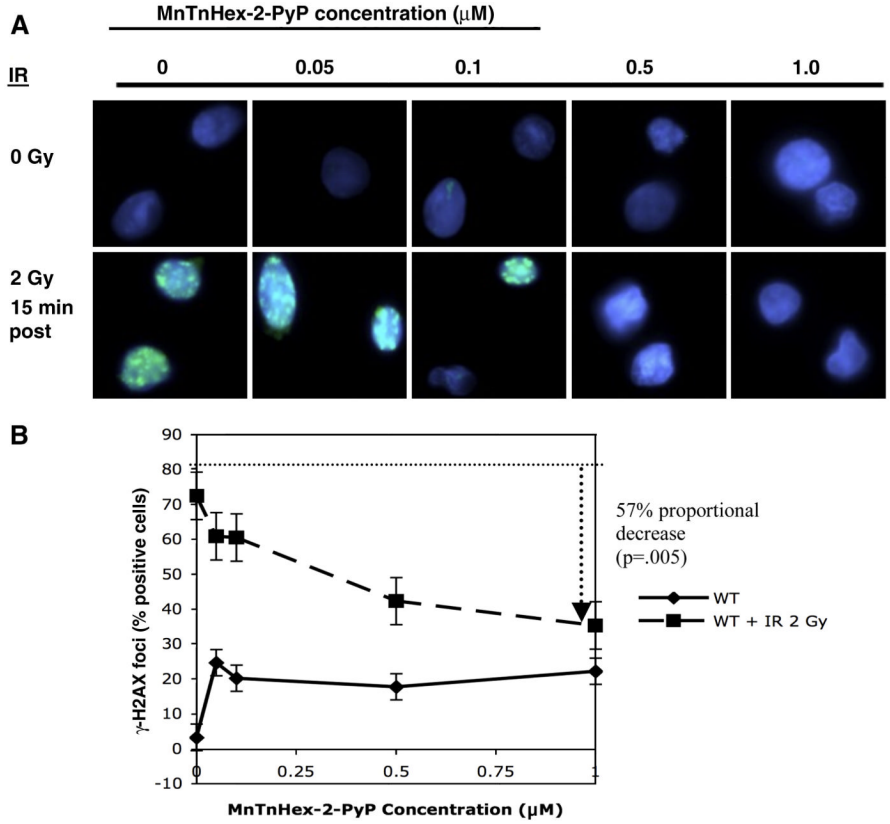

Figure 2.

Gamma-H2AX immunofluorescence foci formation in WT cells. WT cells were incubated in MnTnHex-2-PyP for 18 hours, were irradiated with 2 Gy and fixed with paraformaldehyde onto coverslips. After permeabilization with 0.5% Triton-X 100, cells were stained for γ-H2AX and cells were scored for presence of IRIF nuclear foci. (A) IRIF results for WT cells treated with MnTnHex-2-PyP. Note reduction in IRIF-positive cells with increasing concentrations of MnTnHex-2-PyP. (B) Quantitation of the IRIF results. Solid line: unirradiated WT cells; dashed line: 15 minutes post-2 Gy WT cells. The dotted guideline indicates the percentage of irradiated WT cells positive for IRIFs, in the absence of any compound; the dashed arrow indicates the maximal reduction in IRIF-positive cells after exposure to 1 μM MnTnHex-2-PyP. Error bars represent the standard error. All slides were coded by one individual and read blindly by another. The results shown here are the average results for 3 experiments.

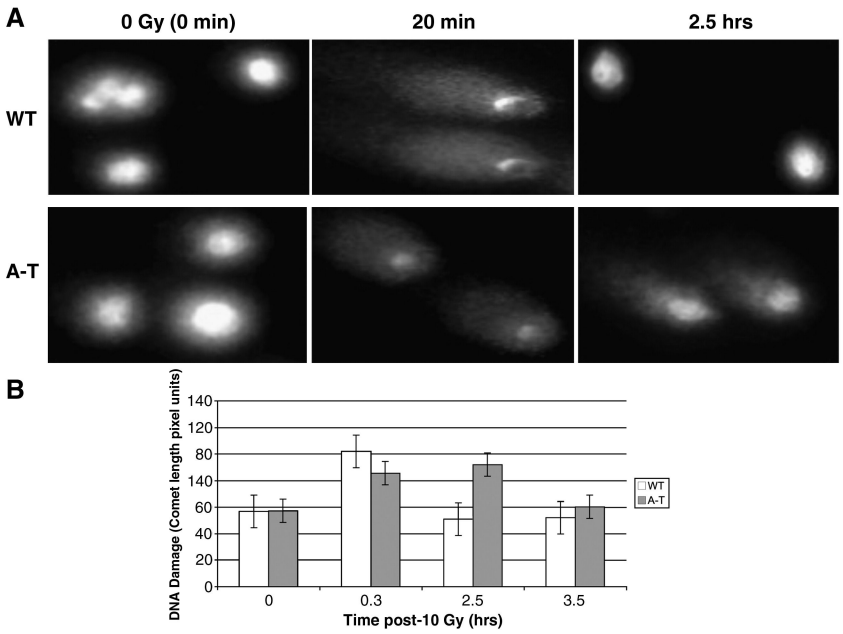

Figure 3.

Delayed DNA double strand break repair in A-T cells assessed by the neutral comet assay. Note return to baseline (i.e. no comets) of WT at 2.5 hrs. Some comets remained at 3.5 hours for A-T cells. (A) The representative comet tails for each time point, in WT and A-T cells, post-10 Gy IR. (B) The quantitation of comet tail length for WT (white column) and A-T cells (gray column). Each data point refers to the average for at least 50 comets and the error bars represent standard errors.

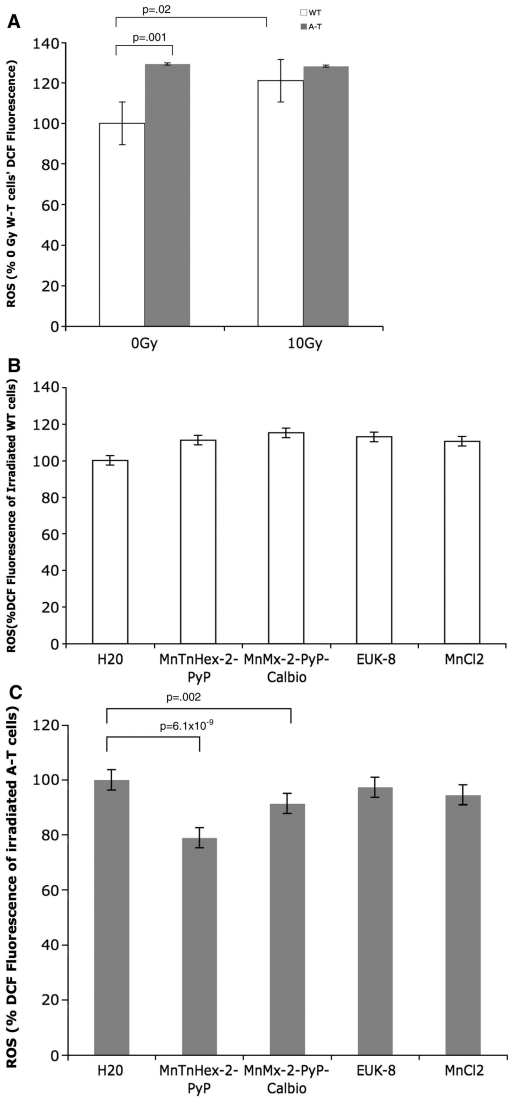

Figure 4.

ROS levels in WT and A-T cells using dichlorofluorescein (DCF) fluorescence. Cells were incubated in 100 μM DCF for 1 hour in PBS at 37°C. Averaged results for 4 separate experiments; error bars represent the standard error. (A) DCF fluorescence 5 minutes after radiation exposure (10 Gy) of WT and A-T cells. Results were normalized to that of unirradiated WT cells. Note increased ROS baseline of A-T cells. (B) Effect of compounds on DCF fluorescence of irradiated (10 Gy) WT cells. Results were normalized to that of irradiated WT cells. (C) Effect of compounds on DCF fluorescence of irradiated (10 Gy) A-T cells. Results were normalized to that of irradiated WT cells. Note antioxidant effects of MnTnHex-2-PyP and MnM_x-2-PyP-Calbio.

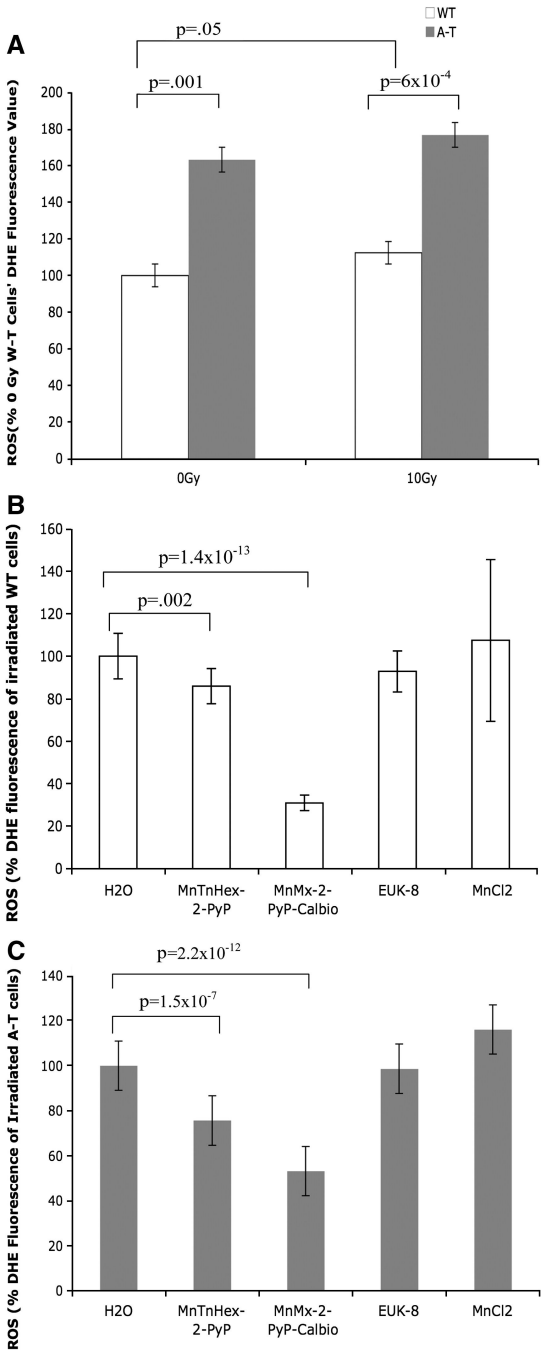

Figure 5.

Superoxide radical formation was detected using dihydroethidium (DHE) fluorescence. Results shown are the averages of for 4 experiments; error bars represent standard errors. (A) DHE fluorescence 5 minutes after 10 Gy in WT and A-T cells. Results were normalized to that of unirradiated WT cells. (B) Effect of compounds on DHE fluorescence in irradiated (10 Gy) WT cells. Results were normalized to that of unirradiated WT cells. (C) Effect of compounds treatment on DHE fluorescence in irradiated (10 Gy) A-T cells. Results were normalized to that of unirradiated A-T cells. Note antioxidant effects for MnTnHex-2-PyP and MnM_x-2-PyP-Calbio on **both** WT and A-T cells.

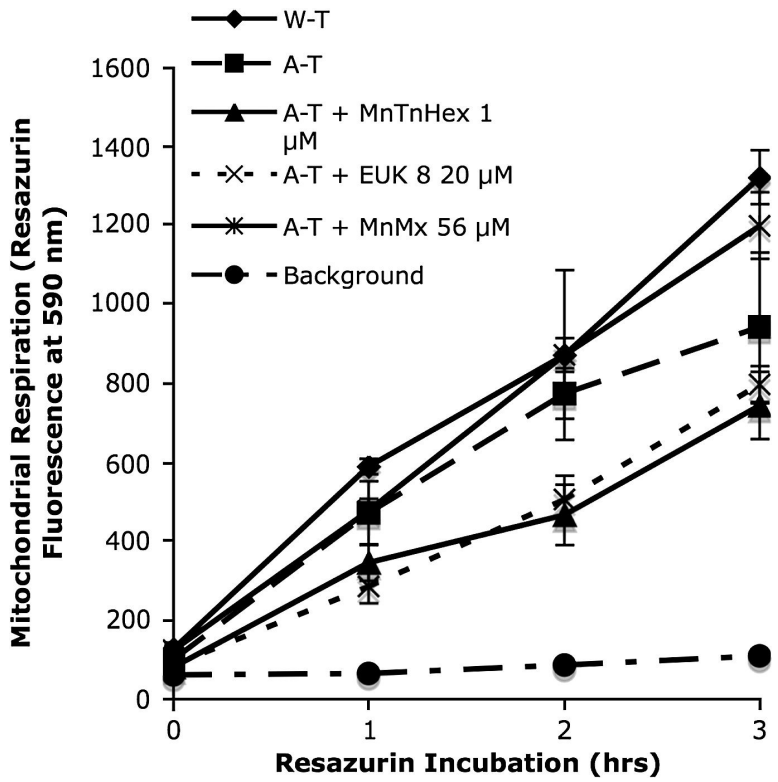

Figure 6.

Mitochondrial respiration measured by resazurin fluorescence. A-T cells exposed to MnM_x-2-Pyp-Calbio show signs of improved mitochondrial function compared to untreated A-T cells. Whereas, A-T cells treated with MnTnHex-2-PyP or EUK-8 showed no effect. Each experiment was done in triplicate. These results are representative of 2 separate experiments and the error bars represent the standard deviations. Note improvement of mitochondrial respiration in A-T cells at 3 hours after addition of resazurin dye.

Table 1

Radioprotective effects of SOD mimics (% Radioprotection)

		XTT				Annexin/Propidium Iodide				Gamma H2AX IRIF		Neutral Comet			
Compound Name	**Conq(μM)**	**WT (%)**	**Stdev**	**A-T (%)**	**Stdev**	**WT (%)**	**Stdev**	**A-T (%)**	**Stdev**	**WT (%)**	**Stdev**	**WT (%)**	**Stdev**	**A-T (%)**	**Stdev**
MnMx-2-PyP-Calbio	56	25*	7.29	−16.23	16.12	11*	2.10	−11.50	9.96	9.96	5.77	19.99*	17.16	0.22	14.05
MnTM-2-PyP	1	−45.74	10.91	−96.22	12.10	9.01	6.26	2.03	9.87	13.69	2.16	8.83*	14.12	0.00	15.89
MnTE-2-PyP	1	−53.33	41.67	41.67	14.29	12.32	3.44	14.21	6.75	2.22	5.51	13.45	10.57	0.00	18.43
MnTnHex-2-PyP	1	58*	7.32	−17.49	56.68	28.61	26.04	39*	3.25	57*	11.31	29.76	16.92	15.43	18.79
MnTTEG-2-PyP	1	−36.71	25.00	−81.81	61.19	3.22	0.41	4.12	10.61	19.53	12.34	18.56	16.28	0.00	14.28
MnBr8TSPP	1	5.35	4.96	−27.81	12.47	−40.58	11.55	−41.56	16.72	70.33	2.65	12.75	10.78	0.00	11.12
EUK-8	20	14.79	45.50	−14.92	14.13	−6.10	12.23	19.56	16.43	−0.43	10.41	27.66	14.61	15.86	16.50
EUK-134	10	−29.57	3.33	−50.81	4.54	7.18	9.97	8*	4.23	52*	4.35	21.02	27.29	0.00	20.23
EUK-189	20	−87.12	61.59	−18.76	4.36	7.25	12.09	10.95	7.82	30.31	7.12	0.00	12.57	0.00	16.14
M40404	20	1.49	12.90	−13.24	21.46	14.31	8.25	4.36	1.63	−60.78	3.24	44.50	12.56	28.04	44.87
M40403	20	−11.04	4.49	−15.78	11.60	33.02	19.96	5.04	4.86	−45.54	3.30	35.66	15.46	0.00	18.75
$MnCl_2$	1	31*	0.55	16.00	12.94	11.69	17.19	−5.12	6.47	22.79	13.00	21.89	20.13	0.00	35.97

[a] % Protection is shown as $\left[\frac{(\text{IR+vehicle}) - (\text{IR+compound−treated})}{(\text{IR+vehicle})} \times 100\%\right]$ Student's t-test was used to measure statistical significance.

* P value ≤ 0.1

Table 2

Thin-layer chromatography as a measure of the lipophilicity of Mn complexes on aluminum silica-gel sheets (EMD Chemicals, Inc, 60 F_{254}), with KNO_3 ($H_2O_{saturated}$):H_2O:acetonitrile= 1:1:8 as a solvent.

Rf	MnTM-2-PyP	MnM_x-2-PyP[a] - Calbio	MnTnHex-2-PyP[b]	MnTE-2-PyP	Mn Salen	Mn Salen	M40403	M40404	$MnCl_2$
1	0.03	0.03	0.38	0.06	0.72	0.94	0.75	0.77	0.00
1		0.07	0.50					0.61	
1		0.24	0.52						
1		0.46							
1		0.63							
Average		**0.29**	**0.46**					**0.69**	

[a] Five R_f values correspond to non-methylated and mono to tetra-methylated species in the mixture of Calbiochem product; the 5 species seem to be present in mixture at similar amounts, the average R_f was given.

[b] 3 R_f values relate to three atropoisomers of MnTnHex-2-PyP; the average values were given so that the lipophilicity of the Mn compounds studied could be compared.

Table 3

Superoxide dismutase activity (log k_{cat}) of the Mn compounds studied

Class	Compound	log k_{cat} (M^{-1} s^{-1})	Reference
Mn porphyrins	MnM_x-2-PyP-Calbio	<6.5.[a]	[60]
	MnTM-2-PyP	7.79	[12]
	MnTE-2-PyP	7.76	[12]
	MnTnHex-2-PyP	7.48	[12]
	MnTTEG-2-PyP	8.11	[13]
	$MnBr_8$TSPP	5.56	[11]
Mn salens	EUK-8	5.78	[20]
	EUK-134	5.78	[19]
	EUK-189	5.78	[19]
Mn cyclic polyamines	M40403	7.08,6.55	[48,67]
	M40404	Inactive	[48]
Control	Mn^{2+}	6.1 – 7.7	[20]

[a]This is not a single compound, but a mixture of several differently *N*-methylated Mn porphyrins that are present in a mixture in approximately same amounts(see text). Thus, the log k_{cat} is likely lower than 6.5 M^{-1} s^{-1} based on the data for tri- (log k_{cat} = 6.63) and di-methylated species (log k_{cat} = 6.52) [60].